General Disclaimer

- This document has been reproduced from the best copy furnished by the organizational source. It is being released in the interest of making available as much information as possible.

- This document may contain data, which exceeds the sheet parameters. It was furnished in this condition by the organizational source and is the best copy available.

- This document may contain tone-on-tone or color graphs, charts and/or pictures, which have been reproduced in black and white.

- This document is paginated as submitted by the original source.

- Portions of this document are not fully legible due to the historical nature of some of the material. However, it is the best reproduction available from the original submission.

NASA Technical Memorandum 87046

Life Cycle Test Results of a Bipolar Nickel Hydrogen Battery

Robert L. Cataldo
Lewis Research Center
Cleveland, Ohio

Prepared for the
20th Intersociety Energy Conversion Engineering Conference (IECEC)
cosponsored by the SAE, ANS, ASME, IEEE, AIAA, ACS, and AIChE
Miami Beach, Florida, August 18–23, 1985

NASA

LIFE CYCLE TEST RESULTS OF A BIPOLAR NICKEL HYDROGEN BATTERY

Robert L. Cataldo
National Aeronautics and Space Administration
Lewis Research Center
Cleveland, Ohio 44135

ABSTRACT

This paper presents a history of low-earth-orbit laboratory test data on a 6.5 Ah bipolar nickel hydrogen battery designed and built at the NASA Lewis Research Center. During the past several years the Storage and Thermal Branch has been deeply involved in the design, development, and optimization of nickel hydrogen devices. The bipolar concept is a means of achieving the goal of producing an acceptable battery of higher energy density, able to withstand the demands of low-earth-orbit regimes.

Over the past several years, the NASA's Lewis Research Center has been actively engaged in the development of a bipolar configured nickel hydrogen battery. Several studies have pointed out that battery simplicity and weight savings can be realized by employing bipolar construction techniques. The actual weight savings compared to conventional nickel hydrogen designs is in the neighborhood of 20 to 30 percent, and is largely dependent on the particular mission and its specific requirement. The aspect of modularity, where the complete system of storage and heat rejection is integrated into one package, provides the ability to accommodate the growing needs of large systems with little or no impact on the whole system.

In August of 1982, a concept verification program was initiated. A 6.5 Ah 10 cell battery was placed on test. The battery was successfully cycled on a low-earth-orbit regime at 80 percent depth-of-discharge for 2000 cycles. At this point the battery was disassembled and components evaluated for early failure mechanisms.

A second battery was assembled in November, 1983 and accrued over 4600 low-earth-orbit cycles prior to battery disassembly.

The remainder of this paper will summarize the performance characteristics of this second stack design.

CELL COMPONENT DESIGN FEATURES

Several special features are incorporated into this battery design that are uncommon to the more conventional nickel hydrogen cells made to date (ref. 1). These features include: electrolyte reservoir plate (ERP) and strategically located recombination sites. The other cell components are more commonly found in other conventional cells. The following describe the composition, manufacture, and function of each cell component, while figure 1 shows the relative positioning of each component within a typical cell housing.

Nickel Electrode

The nickel electrodes used were electrochemically impregnated dry sinters. The electrodes had a screen grid and an active material loading of about 1.60 grams/cc of void volume.

The electrode dimensions were 10.1 cm wide by 21.6 cm long and about 0.1 cm thick. The active area was 218 cm^2 (33.8 in^2). The outer perimeter of the electrode was slightly smaller than the inner dimensions of the cell housing to accommodate any growth encountered during cycling. Flooded capacity tests on a 38.7 cm^2 electrode yielded 2.0 Ah at a current density of 13 mA/cm^2 (c/4). This corresponded to a capacity of 11 Ah for the full scale electrode.

Hydrogen Electrode

The hydrogen electrode was a catalyzed porous screen, non-Teflon backed fuel cell type electrode. The screen or back side of the electrode had no Teflon layer because electrons are conducted normal to the face plane through the gas access screen to the adjacent bipolar plate. The average hydrogen electrode thickness was 0.03 cm and the area was equal to that of the nickel electrode.

Separator

The separator material was a beater treated asbestos (BTA). BTA is a reconstituted blend of asbestos sheets with a 5 percent latex binder. The experimentally determined bubble pressure (pressure at which the first bubble passes through the separator) was 2.0 atm. The dimensions of the separator were 11.9 cm wide by 23.3 cm long, making it larger than the electrodes. This extra separator area, along with six wick rings, formed a seal with the frame ledge to provide a barrier against oxygen passage to the hydrogen electrode (fig. 1). The uncompressed thickness of the separator was 0.053 cm (21 mils), while the average compressed thickness was designed to be 0.025 cm (10 mils).

Electrolyte Reservoir Plate

The electrolyte reservoir plate (ERP) was a foam nickel structure with a density of 10 percent. Each plate was compressed from 0.25 to 0.125 cm, followed by cutting with a rule die that cut out four slots 0.8 cm wide and 20.6 cm long to house the recombination strips. The average pore diameter was 0.025 cm (10 mils). This pore size allowed the passage of hydrogen and oxygen gas through the ERP to the recombination sites. The water vapor, that was formed at the recombination sites during the end of charge, condensed on the nickel foam and was freely wicked out by the separator and nickel electrode. This action aides in electrolyte management, where the goal is to return electrolyte to the equilibrium concentration.

The ERP served as a compression spring element, thereby absorbing expansion of the nickel electrode without significant yielding. This spring-like action can maintain a compressive force on the nickel electrode and possibly reduce the extent of the expansion. Electrolyte, in excess of normal operating

tolerances, was added to the ERP during assembly activation. Sufficient quantities of excess electrolyte was held in the smaller pores of the ERP to accommodate the nickel electrode's electrolyte requirements during cycling. The ERP was also used as a shimming device. The final thickness of the ERP was controlled to trim the total height of the cell components in order to accommodate variances in cell housing dimensions. Therefore, the compression of each cell was made more uniform.

Gas Flow Screen

A screen of expanded nickel was placed behind the hydrogen electrode to facilitate the ingress and egress of hydrogen gas. As in the ERP, an electrically conductive path must exist between the hydrogen electrode and adjacent bipolar plate. Gas channels were provided in the cell housing that aligned with the gas screen. The thickness of the screen was 0.10 cm (0.042 in) with an approximate open area of 95 percent.

Cell Housings

The injection molded polysulfone frames were used to contain the cell components and electrolyte. The nominal frame thickness was 0.378 cm (0.149 in) as shown in figure 1. The inner frame ledge provides a means of sealing the separator around the nickel electrode, thus eliminating evolved oxygen passing to the hydrogen electrode. Hydrogen gas was channeled to the hydrogen electrode via slots connecting the inner frame to two manifolds. The 16 slots provide 0.515 cm^2 of area for hydrogen gas ingress/egress. These slots were in line with the gas flow screen (expanded nickel). Similar slots and manifolding were provided on the other side of the frame to supply hydrogen gas to the recombination sites. The total slot area for this side was 0.296 cm^2 and these slots align with the electrolyte reservoir plate.

Bipolar Plate

The bipolar plates were 0.050 cm (0.020 in) nickel sheets and were sandwiched between each frame. Each cell was enclosed between two bipolar plates. A neoprene gasket fit into a recess in the frame and seals against the bipolar plate, retaining the electrolyte within each cell. External current connections were made to the bipolar terminal plates on each end. The interior bipolar plates conduct current from the positive electrode of one cell to the negative electrode of the next, thus no intercell electrical connectors were needed. However, electrical connections were made to each plate to monitor individual cell voltages. The bipolar plate was also used for heat rejection. Each plate extends beyond the frame on two opposite sides forming a set of cooling fins.

Life Systems Inc. of Beachwood, Ohio has loaned to NASA Lewis Research Center the following hardware: cell frames, stack end plates, insulation plates, tie bolts, and bipolar plates to help expedite the verification testing of the bipolar concept as applied to nickel-hydrogen batteries.

TESTING

The stack was assembled in November of 1983. A series of formation tests were performed to establish an actual battery capacity. The charge ampere-hour input was increased from 8.6 to 9.6 Ah over 13 cycles, charging at 3.75 A for appropriate times. The discharge current, 1.875 A remained the same for each discharge. The ampere-hours discharged to 0.5 V (lowest cell) increased from 7.82 to 8.1 Ah. The nominal capacity asymptotically reached 8.1 Ah as the charge ampere-hours were increased. The capacity discharged to 1.0 V of the weakest cell was 7.8 Ah as shown in table II, and this value was used as "C" for the characterization tests.

The characterization test matrix contained charge rates of C/4, C/2, and C and discharge rates of C/4, C/2, C, and 2C, as well as one 10C discharge. The results are shown on figure 2 and compared to similar results of Build I.

LEO cycling to 80 percent depth of discharge (based on the 1.6 C rate capacity of fig. 2) at the 9.6 A rate was started following the characterization tests. The battery was tested for 4600 cycles before it was taken off-line. During battery cycling, a number of manipulations were done to the battery to improve performance. Changes from Build I were incorporated into Build II involving components, electrolyte activation and compressive loading as noted in table I. These manipulations to the stack were done to discover which changes were the major contributors to the reduced voltage performance noted from comparing Build I to Build II. The following topics discuss some of the more significant events that happened during cycling.

ELECTROLYTE ACTIVATION

The new method of electrolyte activation was to introduce electrolyte as each cell was assembled. The nickel electrodes were vacuum filled and drained with an average take up of 9.3 ml. The ERP received 50 percent by weight (11 ml) and the separator 150 percent by weight (15 ml). These values were obtained from electrolyte retention tests performed on the separator and ERP. The hydrogen electrode was not vacuum filled because the required electrolyte interface would be provided from contact with the separator.

The method used for electrolyte activation on Build I was to pull a vacuum via the stack manifolds and back fill with electrolyte. The use of manifolds for electrolyte activation created a clean up problem in the manifolds which increased the likelihood of developing shunt paths. The severity of the problem becomes significant as battery size is scaled up. In addition, the fixturing of the vacuum/electrolyte system to the battery and the cell housing faces must be sealed to hold a hard vacuum. This can be a difficult task as was our experience with Build I.

Battery voltages were declining over the first 20 LEO cycles. Electrolyte problems were suspected. A vacuum was pulled on the vessel that houses the battery. The end-of-discharge (EOD) voltage increased by 100 mV/cell initially, but was declining at a slower rate and stabilized at 50 mV/cell decrease. The vacuum was thought to have had relocated some electrolyte into the smaller pores of the cell components and partially into the hydrogen electrode. The battery was removed from the vessel and vacuum back filled with electrolyte. This provided higher stabilized EOD voltages. The battery was disassembled to

replace the components of three cells. Cell 2 received a vacuum filled hydrogen electrode and when placed on test it had voltage comparable to the cells that were back filled, thus confirming the need to also vacuum fill the hydrogen electrode.

SHUNT CURRENT TESTING

The need to eliminate shunt currents, caused by electrolyte bridging between the bipolar plates separating each cell, was discovered in Build I. The bipolar plate edges were coated with Teflon to make the cell to cell path hydrophobic. The electrolyte tended to bead up instead of making a continuous liquid path on the Teflon surfaces, thus minimizing electrolyte creepage. Several 72-hr open circuit stands were done to evaluate the Teflon coating. No shunt currents were discovered as in Build I, where a shunt current drained a cell in 50 hr. Therefore, the need for hydrophobic seals and gas passages are necessary to eliminate electrolyte creepage and shunt currents.

DEEP DISCHARGE RECONDITIONING

A performance increase was observed by doing several LEO rate discharges to 0.5 V for the lowest cell. The deep discharge reconditioning made a significant increase in battery voltage for 20 to 30 cycles and also decreased the rate of degradation of EOD voltages.

Several times during cycling the stack was deep discharged and electrically shorted out over night. This procedure also provided marked improvements in EOD voltages. However, these attempts at improving performance were not as effective later on in cycling as it was previously. Possibly a different mode of capacity loss occurred which is not recoverable by deep discharging.

CELL COMPRESSION

After 2800 cycles were run, a 4 mil nickel shim was added to each cell. The shim was added to increase the stack component compression. Compression tests on various materials and separator thicknesses indicated that our stack preload may not have been sufficient to compress the separator and provide good contact with the bipolar plate. Table III shows the individual cell voltages for over 300 cycles prior to and after the installation of the shims. It is of interest to note that all the cells had declined in EOD voltage prior to the shim installation; however, six cells increased and four cells decreased in voltage afterward. Again the results are not clear about the merit of increased compression. It is possible the cells with reduced voltage have been over compressed, which may have forced electrolyte from the active areas.

CAPACITY MEASUREMENTS

Table II displays the C/4 capacities measured to 1.0 V throughout battery cycling. A loss in capacity is noted in all cells. Cell 6 has experienced the greatest decline - 35 percent - while the other cells have degraded about 30 percent. The nickel electrode removed from cell 10 at 2800 cycles, measured a loss of about 15 percent in capacity at C/4 rates and 25 percent at the 2C rate in flooded capacity tests while the electrodes under cell conditions at 3350 cycles showed a 20 percent decrease. In the span of cycles 3100 to 3860

the depth of discharge was adjusted to 70 percent corresponding to their original capacity as noted in figure 3. Following the last C/4 capacity discharges at cycle 3906, the depth of discharge was resumed to the 80 percent level. The ampere-hours discharged was almost 90 percent of the current actual electrode capacity.

SHORTED CELL AND OVERCHARGE CAPABILITIES

Following a 72 hr self-discharge test after 4075 LEO cycles, cells 6, 7, and 10 had zero volts. The battery was drained at the 1.0 and 0.5 A rate and shorted overnight. Cells 6 and 7 recovered normal cell voltage after charge but cell 10 did not recover. The battery was cycled with cell 10 shorted to observe operational behavior. Twenty-five cycles were completed with a watt-hour efficiency loss of about 2 percent. This loss would be reduced to 0.2 percent in a full 120 V battery.

For the next 16 cycles, a malfunctioning discharge load caused the battery to receive full, 1 hr charges with the battery on open circuit for the half hour discharge time. Battery temperatures reached 57 °C at end of charge and cooled to 35 °C after the half hour. No apparent problems occurred due to the successive overcharges. Because normal cycling was continued with no anomalies in voltage performance noted.

The shorted cell was removed from the stack and the remaining cells were cycled. The analysis of cell 10 showed evidence of high compression, where the impression of the gas screen could be readily seen in the hydrogen electrode and separator. An obvious shorting of the nickel and hydrogen electrodes through the separator occurred. The points of contact were aligned with the two ends of one of the recombination strips. The nickel electrode in these two areas was protruding toward the hydrogen electrode and the deflection was about 0.025 cm (0.010 in).

Over 500 additional cycles were run on the nine cells before problems occurred with three cells - 7, 8, and 9. During charging cell 9 had an end-of-discharge voltage of 1.3 V, about 0.250 mV below the normal value. The voltage dropped to below 0.6 V as soon as charging stopped. This action placed the test facility in a standby mode. Continued data transmissions recorded the voltage decline of cells 7 and 8. Cell 7's voltage reduced to 0 V after 2 hr of open circuit. Testing was terminated and the battery disassembled for analysis.

POST TEST INSPECTION

Visual inspection of the cells during teardown revealed several items that are of particular concern.

(1) The porous Teflon membrane that surrounded each recombination strip had reduced in size enough to expose the recombination strip on several sites in cells 3, 7, 8, and 9.

(2) Some nickel electrodes developed humps in the areas correlating with the ends of the recombination strips. These humps were directed toward the ERP and were raised above the electrode surface 0.07 cm (0.030 in) to 0.01 cm (0.040 in), and approximately 0.64 cm (0.250 in) by 0.64 cm (0.250 in) in area.

(3) The hydrogen electrodes were pressed into the expanded metal gas screen with sufficient compression to reveal the pattern and texture of the gas screen.

The humping of the nickel electrode back toward the ERP probably touched the exposed ends of the recombination site. This action caused a parasitic reaction to occur, which can diminish charge capacity and discharge capacity. This problem could explain the low end-of-charge voltage of cells 8 and 9 and the voltage decline of cell 7 previously mentioned. Additional testing verified this, where the Teflon tube reduced in size when heated in an oven and a loss in capacity of nearly 50 percent was noted when a section of hydrogen electrode was placed in contact with the nickel electrode.

The gas screen used in this Build was similar to that of Build I, however, the screen used in Build I was a stock size of 0.15 cm (.060 in) compressed to 0.11 cm (0.043 in), where in Build II the stock size of the screen was 0.12 cm (0.045 in) compressed to 0.11 cm (0.043 in). Compressing the screen tends to rollover the sharper points. However, this screen was slightly compressed, thus the sharper points made the indentations in the hydrogen electrode with less compression.

CONCLUSIONS

Much helpful and interesting data was generated during the cycling of this battery at the stressful rate of 80 percent depth-of-discharge. Over 4600 cycles were achieved on a unique battery design for nickel hydrogen systems. Watt-hour efficiencies in the 75 percent range have been demonstrated. The capability of overcharge has been shown were over 500 cycles were run following the successive charges. Most likely these overcharges resulted in failure of some cells where the Teflon tubes shrank due to high heat generated on overcharge. However, other cells did not experience these problems. The preheating of the Teflon tubes will eliminate this problem and make the battery more tolerant to abnormal operating conditions.

Testing of cell components, recombination site analysis and cell compression are being evaluated in small scale screening test and compared to full scale life test results. The combination of these test results will be correlated and evaluated in generating a generic standard bipolar design that can be tailored to specific mission requirements with only minor alterations.

REFERENCE

1. Cataldo, R.L.: Test Results for a Ten Cell Bipolar Nickel-Hydrogen Battery, 18th IECEC Proceedings, NASA TM-83384.

TABLE I. - SUMMARY OF DESIGN DIFFERENCES OF BUILD I AND BUILD II DESIGNS

Component	Build I	Build II
Nickel electrode	Chemically loaded 2.1 g/cc	Electrochemically loaded 1.6 g/cc
Hydrogen Electrode	Fuel cell type Nonbacked	Fuel cell type Nonbacked
Separator	Asbestos 21 mils 5% binder	Asbestos 14 mils 5% binder
Electrolyte reservoir	Nickel foam	Nickel foam
Recombination sites	H_2 electrode Open gortex	H_2 electrode Sealed gortex
Bipolar plate	Gold plated nickel	Gold removed, Teflon coated edges
Activation process	Vacuum back fill with KOH drain	Vacuum fill nickel electrodes; metered amount added to each cell

TABLE II. - DISCHARGE CAPACITIES TO 1.0 V AT THE C/4 RATE OF 1.9 A

Cycle no.	Cell Number									
	1	2	3	4	5	6	7	8	9	10
[e]16	[a]7.8	[b]8.0	[b]8.0	[b]8.0	[b]8.0	[b]8.0	[b]8.0	[b]8.0	[b]8.0	[b]8.0
[c]2363	5.76	5.76	5.73	5.82	5.9	5.7	5.7	5.9	[a]5.6	5.7
[c]2364	6.7	6.7	[a]6.3	6.45	6.74	6.74	7.0	6.9	7.0	7.0
[d]3350	[b]6.5	6.34	6.34	[a]6.5	[b]6.5	5.93	5.85	6.47	[b]6.5	[b]6.5
[d]3862	[b]5.9	5.8	[a]5.7	5.8	[b]5.9	5.2	5.6	5.7	[b]5.9	[b]5.9
[d]3900	[b]5.6	5.55	[a]5.4	5.5	[b]5.6	5.0	5.23	5.3	[b]5.6	[b]5.6

[a]First cell to reach 0.5 V.
[b]Cells not reaching 1.0 V before event a.
[c]Charge; 8 Ah; 4 A for 2 hr.
[d]Charge; normal LEO cycle interruption.
[e]Charge; 9.1 Ah.

TABLE III. - CELL VOLTAGES BEFORE AND AFTER ADDING A 4 M11 SHIM TO EACH CELL

Cell no.	Without shim			With shim		
	2410	2800	Change	2807	3167	Change
	Volts			Volts		
1	1.173	1.129	-0.044	1.123	1.162	+0.039
2	1.164	1.125	- .039	1.122	1.117	- .005
3	1.156	1.095	- .061	1.096	1.031	- .065
4	1.192	1.145	- .047	1.138	1.158	+ .020
5	1.209	1.173	- .036	1.166	1.187	+ .021
6	1.175	1.112	- .063	1.102	1.109	+ .007
7	1.192	1.139	- .053	1.133	1.026	+ .107
8	1.139	1.097	- .042	1.092	1.074	- .018
9	1.186	1.127	- .059	1.125	1.154	+ .029
10	1.168	1.121	- .047	1.112	1.178	+ .066
Net change			-0.491			-0.013

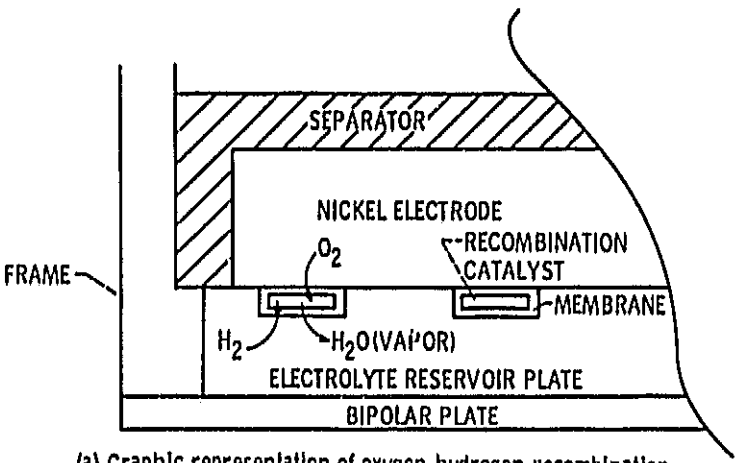

(a) Graphic representation of oxygen hydrogen recombination.

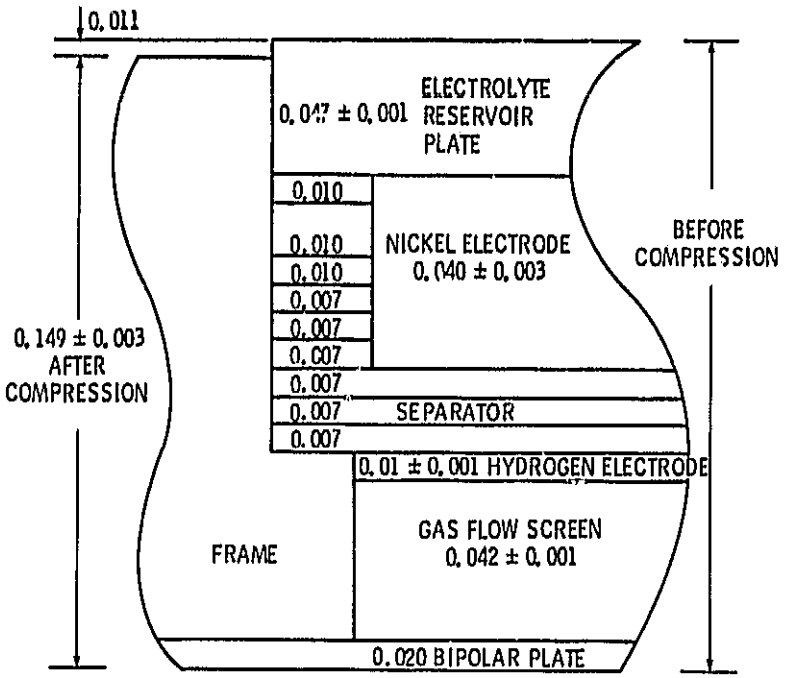

(b) Cell cross section with dimensions of components. (All dimensions are in inches.)

Fig. 1.

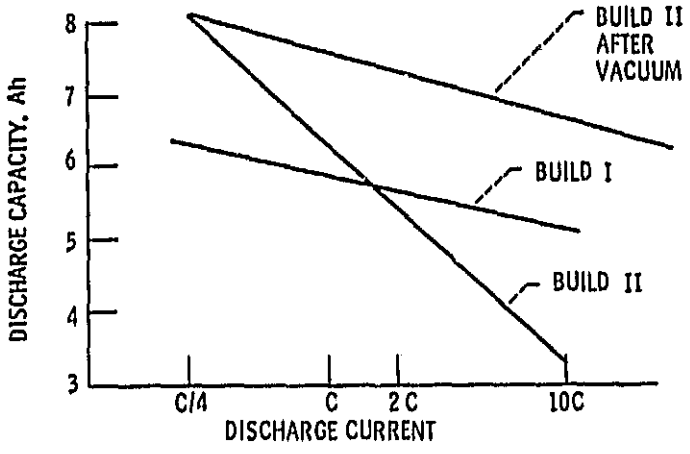

Fig. 2. - Discharge capacity versus current rate.

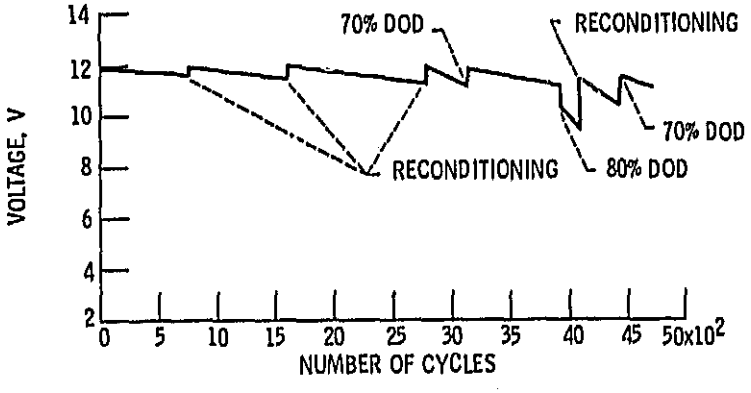

Fig. 3. - End of discharge voltage versus cycles.

1. Report No.	2. Government Accession No.	3. Recipient's Catalog No.
NASA TM-87046		

4. Title and Subtitle	5. Report Date
Life Cycle Test Results of a Bipolar Nickel Hydrogen Battery	6. Performing Organization Code: 506-55-52
7. Author(s): Robert L. Cataldo	8. Performing Organization Report No.: E-2608
	10. Work Unit No.
9. Performing Organization Name and Address: National Aeronautics and Space Administration, Lewis Research Center, Cleveland, Ohio 44135	11. Contract or Grant No.
12. Sponsoring Agency Name and Address: National Aeronautics and Space Administration, Washington, D.C. 20546	13. Type of Report and Period Covered: Technical Memorandum
	14. Sponsoring Agency Code

15. Supplementary Notes

Prepared for the 20th Intersociety Energy Conversion Engineering Conference (IECEC), cosponsored by the SAE, ANS, ASME, IEEE, AIAA, ACS, AICHE, Miami Beach, Florida, August 18-23, 1985.

16. Abstract

This paper presents a history of low-earth-orbit laboratory test data on a 6.5 Ah bipolar nickel hydrogen battery designed and built at the NASA Lewis Research Center. During the past several years the Storage and Thermal Branch has been deeply involved in the design, development, and optimization of nickel hydrogen devices. The bipolar concept is a means of achieving the goal of producing an acceptable battery of higher energy density, able to withstand the demands of low-earth-orbit regimes.

17. Key Words (Suggested by Author(s))	18. Distribution Statement
Battery; Bipolar; Nickel hydrogen test data	Unclassified - unlimited STAR Category 44

19. Security Classif. (of this report)	20. Security Classif. (of this page)	21. No. of pages	22. Price*
Unclassified	Unclassified		

*For sale by the National Technical Information Service, Springfield, Virginia 22161